Supplementary Material for “THC exposure is reflected in the microstructure of the cerebral cortex and amygdala of young adults”

Ryan P. Cabeen, John M. Allman, Arthur W. Toga

19 March, 2020

Contents

This document provides supplementary material for the manuscript entitled “*THC exposure is reflected in the microstructure of the cerebral cortex and amygdala in young adults*”. We first present demographic information about participant age, gender, body mass index, and behavioral characteristics, as well as a statistical summary of how these variables relate to THC exposure. We then examine diffusion MRI microstructure parameters with respect to THC exposure as measured by a urine screen, showing raw data plots and results from multiple linear regression modeling. We then present results from an analagous comparison with self-reported cannabis usage showing dose-dependency using non-parametric regression plots. Following this, we compare of a general factor of microstructure with behavioral characterisics using multiple linear regression and logistic regression modeling. We report findings that relate to some specific brain areas and imaging metrics that were not presented in the manuscript due to space limitations, and these pieces are briefly summarized below. While the manuscript focused on dispersion, we include results from diffusion tensor imaging fractional anisotropy (**FA**) and the NODDI orientation dispersion index (**ODI**). The following brain areas were analyzed: frontoinsular cortex (**FIC**), anterior agranular insular cortex (**AAIC**), amygdala lateral portion of the basolateral nucleus (**BLN_La**), amygdalostriatal transition areas (**ATA_ASTA**), and amygdala intercalated nucleus (**INA**). We also include a composite metric for ventromedial prefrontal cortex **vmPFC**, which is the average of Brodmann areas p32, d32, 10r, and a24. Unless identified otherwise, all measures are averages of parameters the left and right hemispheres. We also included a general factor summarizing FA and ODI microstructure parameters (**FA_GEN_FAC** and **ODI_GEN_FAC** respectively); these were obtained by principal component analysis of the above brain areas and by defining the general factor by the scores associated with the first component. We denote the results of the THC urine screen with the binary variable **THC**, and also analysis several other variables of interest: age, gender, body mass index (**BMI**), memory accuracy measured using the NIH Toolbox memory tests (**MEM**), self-reported paternal substance abuse (**PSA**), self reported daily drinking (**DailyDrink**), self reported daily smoking (**DailySmoke**), self-reported aggregate cannabis usage (**CannabisDose**). We also operationalized negative intrusive thinking (**NIT**) using the thought problems scale from the Achenbach System of Empirically Based Assessment (ASEBA), which has been found to be associated with a variety of psychotic disorders. The scale consists of a ten item questionnaire, which covers intrusive thoughts, nervous ticks, self-harm and accidental injury, auditory and visual hallucinations, and repetitive behavior.

Summary of Demographic Variables and Relation to THC

Shown below are plots and tables reporting the data distribution of participants' age, gender, body mass index (BMI), negative intrusive thinking (NIT), memory accuracy (MEM) self-reported cannabis use (Cannabis-Dose), and THC exposure as measured from a urine screen (THC).

The results show that the THC urine screen largely agreed with the self-reported cannabis usage, and THC exposure showed a significant relationship with memory accuracy, negative intrusive thinking, and gender.

Plots of the distribution of demographic variables

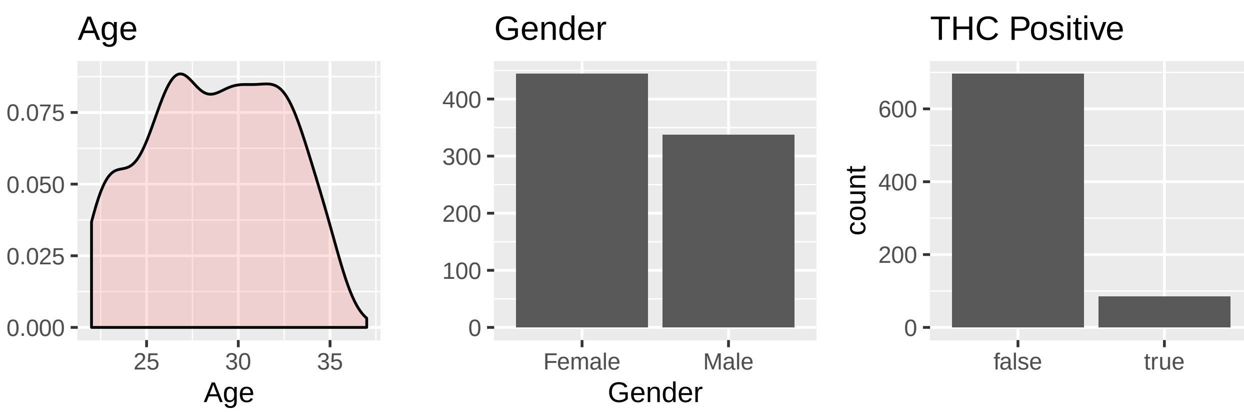

Figure 1: Plots showing the distribution of participant ages, genders, and positive results from the THC test

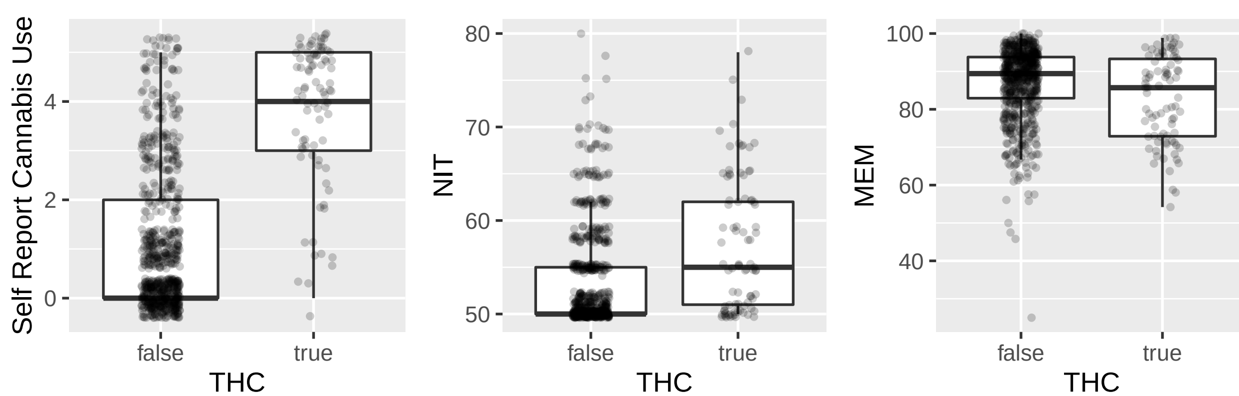

Figure 2: Plots showing the relationship between THC exposure and self reported usage, ASR thought problems, and memory performance

Table of the distribution of demographic variables

Table 1: A table reporting participant demographics split by THC exposure

	THC	N	Missing	Mean	SD	Min	Q1	Median	Q3	Max
Age	false	696	0	28.84	3.65	22.00	26.00	29.00	32.00	36.00
	true	85	0	27.59	3.72	22.00	25.00	27.00	30.00	37.00
BMI	false	695	1	26.50	5.18	16.65	22.80	25.39	29.33	47.76
	true	85	0	26.61	5.68	18.44	23.04	25.69	29.37	45.17
CannabisDose	false	696	0	1.10	1.47	0.00	0.00	0.00	2.00	5.00
	true	85	0	3.82	1.42	0.00	3.00	4.00	5.00	5.00
NIT	false	693	3	53.25	5.22	50.00	50.00	50.00	55.00	80.00
	true	85	0	57.36	7.21	50.00	51.00	55.00	62.00	78.00
MEM	false	694	2	86.99	9.35	25.00	82.89	89.42	93.78	100.00
	true	83	2	82.68	11.45	54.20	72.88	85.70	93.30	98.83
DailySmoke	false	694	2	0.77	2.05	0.00	0.00	0.00	0.00	7.00
	true	85	0	2.82	3.17	0.00	0.00	1.00	7.00	7.00
DailyDrink	false	694	2	1.55	1.72	0.00	0.00	1.00	2.00	7.00
	true	85	0	2.04	2.08	0.00	0.00	2.00	3.00	7.00

Tests of the relation between THC and demographic variables

Table 2: Multiple linear regression models relating demographic variables to THC exposure, controlling for age and gender

	Dependent variable:					
	Age	MEM	NIT	CannabisDose	DailyDrink	DailySmoke
	(1)	(2)	(3)	(4)	(5)	(6)
THCtrue	−0.245**	−0.578***	0.675***	2.649***	0.382*	1.996***
	p = 0.033	p = 0.00000	p = 0.000	p = 0.000	p = 0.063	p = 0.000
GenderMale	−0.361***	0.324***	0.029	0.357***	0.454***	0.370**
	p = 0.00000	p = 0.00001	p = 0.690	p = 0.002	p = 0.001	p = 0.024
Age		−0.123***	−0.146***	0.051	0.060	0.118
		p = 0.001	p = 0.00004	p = 0.338	p = 0.351	p = 0.143
Constant	0.182***	−0.079*	−0.087*	0.951***	1.367***	0.615***
	p = 0.0002	p = 0.096	p = 0.066	p = 0.000	p = 0.000	p = 0.000
Observations	781	777	778	781	779	779
R^2	0.042	0.066	0.074	0.263	0.023	0.086
Adjusted R^2	0.040	0.062	0.071	0.260	0.019	0.082
Note:						*p<0.1; **p<0.05; ***p<0.01

THC and microstructure in the cerebral cortex and amygdala

Shown below are tables and plots summarizing the relationship between THC exposure and tissue microstructure in the cerebral cortex and amygdala. The tables report the results of multiple linear regression modeling, focusing on the parameters associated with THC exposure, including the change in BIC (dbic) and change in R^2 when from adding THC to the model. Please see the manuscript for details about model construction. Results from individual brain areas and two different diffusion metrics are include: orientation dispersion index (ODI) and fractional anisotropy (FA). We also included a general factor summarizing all significant brain areas (GEN_FAC), which was created using a principal component analysis. The plots include jittered points to show each individual and box plots to show the median and quartiles.

The results show differences among brain areas and hemispheres, and in particular, that ODI typically showed a stronger effect than FA, and the general factor showed the strongest effect overall. FA showed associations in the opposite direction of ODI, which is to be expected given that increased dispersion is understood to decrease tensor anisotropy.

Tests of orientation dispersion

	name	dbic	rsq	arsq	darsq	beta	stde	tval	pval
1	ODI_FIC	11.0	0.073	0.069	0.020	0.501	0.119	4.2	0.00003
2	ODI_AAIC	8.0	0.111	0.106	0.016	0.443	0.116	3.8	0.00014
3	ODI_vmPFC	8.0	0.090	0.084	0.016	0.448	0.117	3.8	0.00014
4	ODI_BAp32	6.5	0.040	0.037	0.015	0.435	0.120	3.6	0.00030
5	ODI_BAs32	0.1	0.105	0.098	0.007	0.302	0.117	2.6	0.00994
6	ODI_BAa24	1.1	0.056	0.052	0.008	0.330	0.118	2.8	0.00547
7	ODI_BA10r	1.3	0.029	0.025	0.009	0.339	0.120	2.8	0.00482
8	ODI_BLN_La	7.4	0.062	0.057	0.016	0.447	0.119	3.8	0.00018
9	ODI_ATA_ASTA	-0.9	0.073	0.068	0.006	0.280	0.117	2.4	0.01729
10	ODI_INA	2.7	0.043	0.038	0.010	0.362	0.119	3.0	0.00237
11	ODI_GEN_FAC	18.0	0.124	0.119	0.027	0.573	0.115	5.0	0.00000

Table 3: Table showing associations between THC exposure and ODI averaged across hemispheres. Each row represents a multiple linear regression model and reports the effect of THC

	name	dbic	rsq	arsq	darsq	beta	stde	tval	pval
1	ODI_FIC_L	1.1	0.040	0.036	0.008	0.334	0.120	2.8	0.00547
2	ODI_FIC_R	11.8	0.076	0.070	0.022	0.518	0.120	4.3	0.00002
3	ODI_AAIC_L	3.7	0.054	0.050	0.012	0.383	0.119	3.2	0.00134
4	ODI_AAIC_R	4.7	0.114	0.109	0.012	0.389	0.115	3.4	0.00079
5	ODI_vmPFC_L	3.0	0.057	0.051	0.011	0.372	0.120	3.1	0.00200
6	ODI_vmPFC_R	4.0	0.084	0.077	0.012	0.385	0.118	3.3	0.00116
7	ODI_BAp32_L	-1.6	0.033	0.030	0.005	0.259	0.116	2.2	0.02500
8	ODI_BAp32_R	5.4	0.035	0.030	0.014	0.418	0.120	3.5	0.00053
9	ODI_BAs32_L	-4.2	0.066	0.060	0.002	0.185	0.118	1.6	0.11762
10	ODI_BAs32_R	1.3	0.071	0.065	0.009	0.325	0.115	2.8	0.00491
11	ODI_BAa24_L	1.4	0.041	0.036	0.009	0.327	0.115	2.8	0.00463
12	ODI_BAa24_R	-1.1	0.060	0.055	0.006	0.279	0.118	2.4	0.01839
13	ODI_BA10r_L	4.0	0.040	0.036	0.012	0.392	0.120	3.3	0.00116
14	ODI_BA10r_R	-5.5	0.003	0.001	0.000	0.130	0.120	1.1	0.27853

Table 4: Table showing associations between THC exposure and ODI seperately in each hemisphere. Each row represents a multiple linear regression model and reports the effect of THC.

Tests of fractional anisotropy

	name	dbic	rsq	arsq	darsq	beta	stde	tval	pval
1	FA_FIC	7.9	0.029	0.027	0.018	-0.459	0.120	-3.8	0.00014
2	FA_AAIC	8.4	0.067	0.064	0.018	-0.461	0.119	-3.9	0.00011
3	FA_vmPFC	-3.4	0.005	0.002	0.003	-0.219	0.123	-1.8	0.07557
4	FA_BAp32	-4.6	0.017	0.013	0.001	-0.169	0.121	-1.4	0.16100
5	FA_BAs32	-2.5	0.020	0.016	0.004	-0.245	0.120	-2.0	0.04197
6	FA_BAa24	-1.2	0.010	0.007	0.006	-0.284	0.122	-2.3	0.02071
7	FA_BA10r	-4.8	0.025	0.021	0.001	-0.157	0.116	-1.3	0.17906
8	FA_BLN_La	10.6	0.041	0.037	0.020	-0.494	0.119	-4.2	0.00003
9	FA_ATA_ASTA	-3.0	0.032	0.027	0.003	-0.228	0.120	-1.9	0.05721
10	FA_INA	1.1	0.028	0.025	0.009	-0.322	0.115	-2.8	0.00536
11	FA_GEN_FAC	16.7	0.063	0.059	0.029	-0.589	0.122	-4.8	0.00000

Table 5: Table showing associations between THC exposure and FA averaged across hemispheres. Each row represents a multiple linear regression model and reports the effect of THC.

	name	dbic	rsq	arsq	darsq	beta	stde	tval	pval
1	FA_FIC_L	1.2	0.030	0.027	0.009	-0.338	0.120	-2.8	0.00514
2	FA_FIC_R	14.4	0.036	0.033	0.026	-0.544	0.118	-4.6	0.00000
3	FA_AAIC_L	5.9	0.043	0.039	0.015	-0.424	0.120	-3.5	0.00041
4	FA_AAIC_R	5.1	0.053	0.049	0.013	-0.405	0.118	-3.4	0.00062
5	FA_vmPFC_L	-5.7	0.014	0.011	-0.000	-0.107	0.116	-0.9	0.35418
6	FA_vmPFC_R	-1.8	0.007	0.004	0.005	-0.265	0.121	-2.2	0.02892
7	FA_BAp32_L	-4.7	0.031	0.027	0.001	-0.159	0.114	-1.4	0.16344
8	FA_BAp32_R	-3.8	0.004	0.002	0.002	-0.203	0.120	-1.7	0.09258
9	FA_BAs32_L	-4.6	0.009	0.007	0.001	-0.165	0.115	-1.4	0.15102
10	FA_BAs32_R	0.2	0.022	0.019	0.007	-0.300	0.115	-2.6	0.00901
11	FA_BAa24_L	-5.3	0.004	0.001	0.000	-0.139	0.122	-1.1	0.25353
12	FA_BAa24_R	-2.3	0.020	0.016	0.004	-0.251	0.120	-2.1	0.03742
13	FA_BA10r_L	-4.7	0.033	0.029	0.001	-0.159	0.115	-1.4	0.16717
14	FA_BA10r_R	-6.0	0.004	0.001	-0.001	-0.090	0.117	-0.8	0.44631

Table 6: Table showing associations between THC exposure and FA seperately in each hemisphere. Each row represents a multiple linear regression model and reports the effect of THC.

Plots of orientation dispersion results

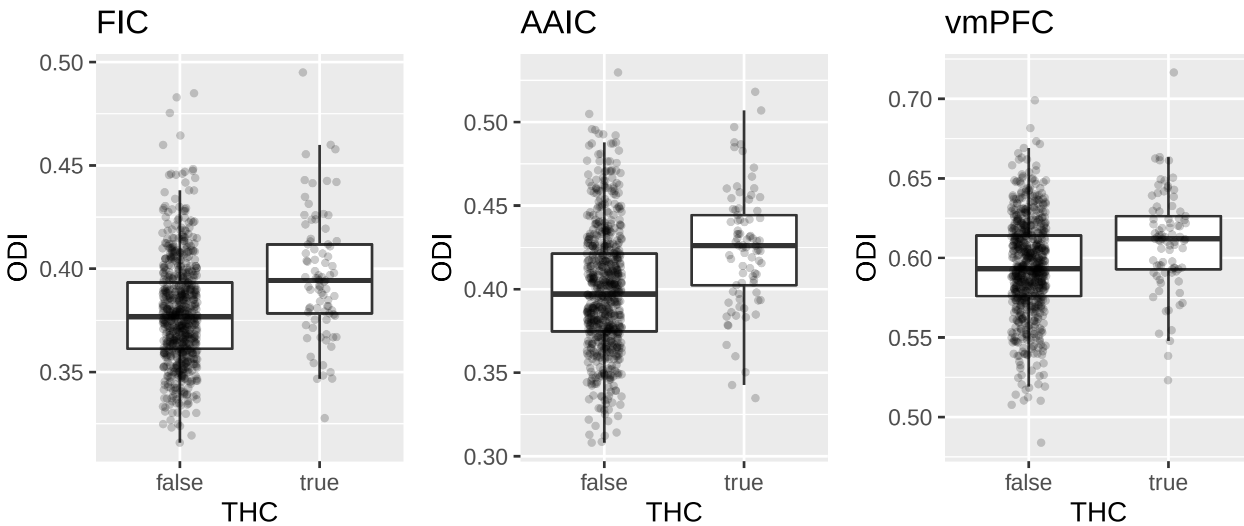

Figure 3: Plots showing cortical ODI measurements as they relate to THC exposure. Each jittered point represents an individual, and the box plot depicts the median and low/high quartiles.

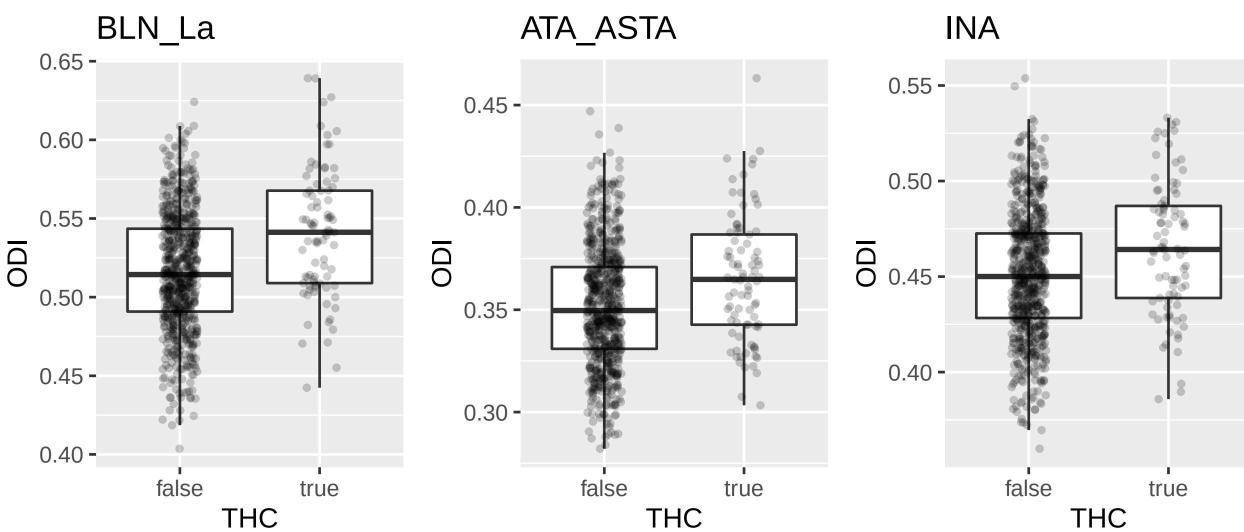

Figure 4: Plots showing amygdala ODI measurements as they relate to THC exposure. Each jittered point represents an individual, and the box plot depicts the median and low/high quartiles.

Plots of fractional anisotropy

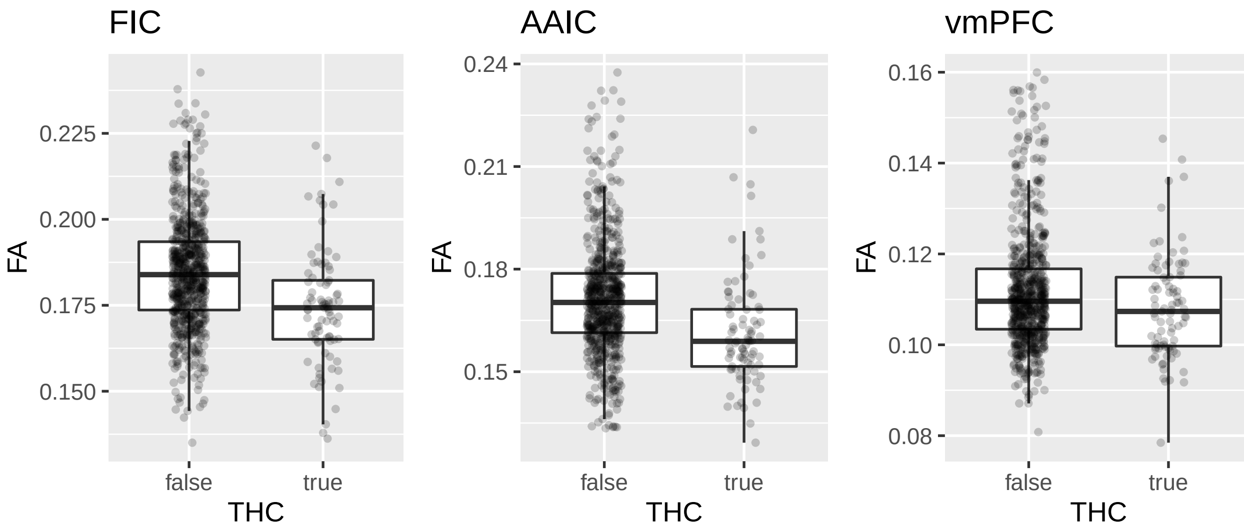

Figure 5: Plots showing cortical FA measurements as they relate to THC exposure. Each jittered point represents an individual, and the box plot depicts the median and low/high quartiles.

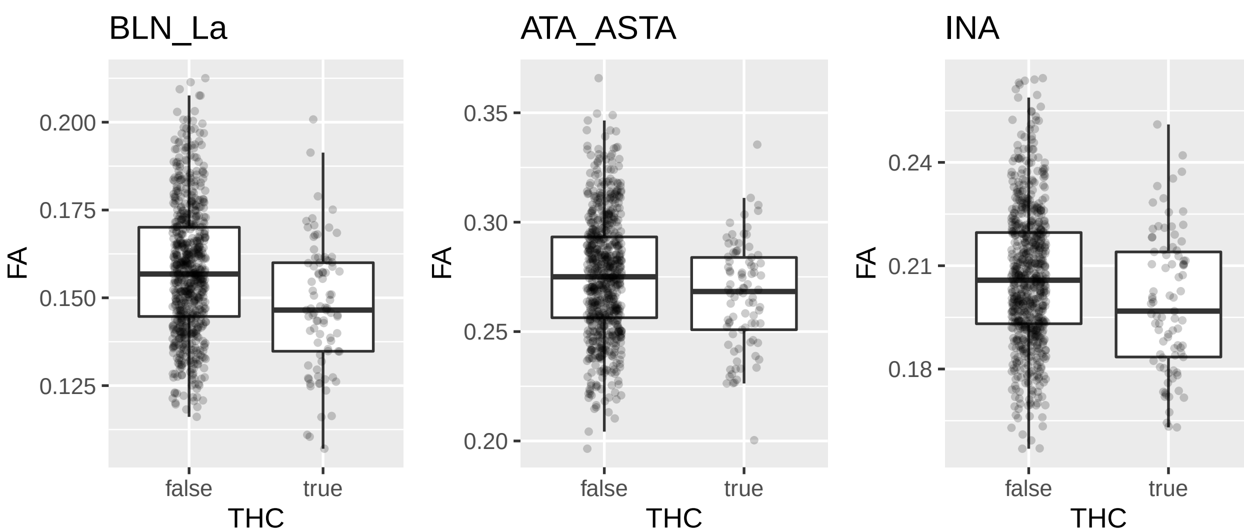

Figure 6: Plots showing amygdala FA measurements as they relate to THC exposure. Each jittered point represents an individual, and the box plot depicts the median and low/high quartiles.

Self-reported cannabis usage and microstructure in the cerebral cortex and amygdala

Shown below are tables and plots describing the relationship between self-reported cannabis usage (CannabisDose) and tissue microstructure. The CannabisDose scale was measured according with the following levels: never used = 0; 1-5 = 1; 6-10 148 = 2; 11-101 = 3; 101-999 = 4; 1000 or more = 5. We performed linear regression modeling of CannabisDose with several tissue microstructure parameters, and we created non-parametric regression plots showing the ODI and FA for each discrete level of the self report.

The results show strong and significant associations between CannabisDose and microstructure in the same direction as the urine screen; however, the urine screen showed a substantially larger effect size. The plots show a non-linear trend, with the two highest usage levels corresponding to the greatest difference in microstructure. Similar to the urine screen, FA showed the opposite trend from ODI. Note: we observed a consistent dip/bump at the second and third levels, which we hypothesize is more related to the nature of self-report than neurobiology.

Table 7: Multiple linear regression plots showing the relation between ODI and self-reported cannabis use

	Dependent variable:				
	ODI_FIC	ODI_AAIC	ODI_vmPFC	ODI_BLN_La	ODI_GEN_FAC
	(1)	(2)	(3)	(4)	(5)
CannabisDose	0.093***	0.091***	0.082***	0.103***	0.122***
	p = 0.00001	p = 0.00002	p = 0.0001	p = 0.00001	p = 0.000
Observations	781	781	781	781	781
R^2	0.025	0.024	0.019	0.030	0.043
Adjusted R^2	0.024	0.023	0.018	0.029	0.041
Note:					*p<0.1; **p<0.05; ***p<0.01

Table 8: Multiple linear regression plots showing the relation between FA and self-reported cannabis use

	Dependent variable:				
	FA_FIC	FA_AAIC	FA_vmPFC	FA_BLN_La	FA_GEN_FAC
	(1)	(2)	(3)	(4)	(5)
CannabisDose	−0.090***	−0.084***	−0.047**	−0.095***	−0.096***
	p = 0.00002	p = 0.0001	p = 0.026	p = 0.00001	p = 0.00001
Observations	781	781	781	781	781
R^2	0.023	0.020	0.006	0.026	0.026
Adjusted R^2	0.022	0.019	0.005	0.024	0.025
Note:					*p<0.1; **p<0.05; ***p<0.01

Plots of orientation dispersion

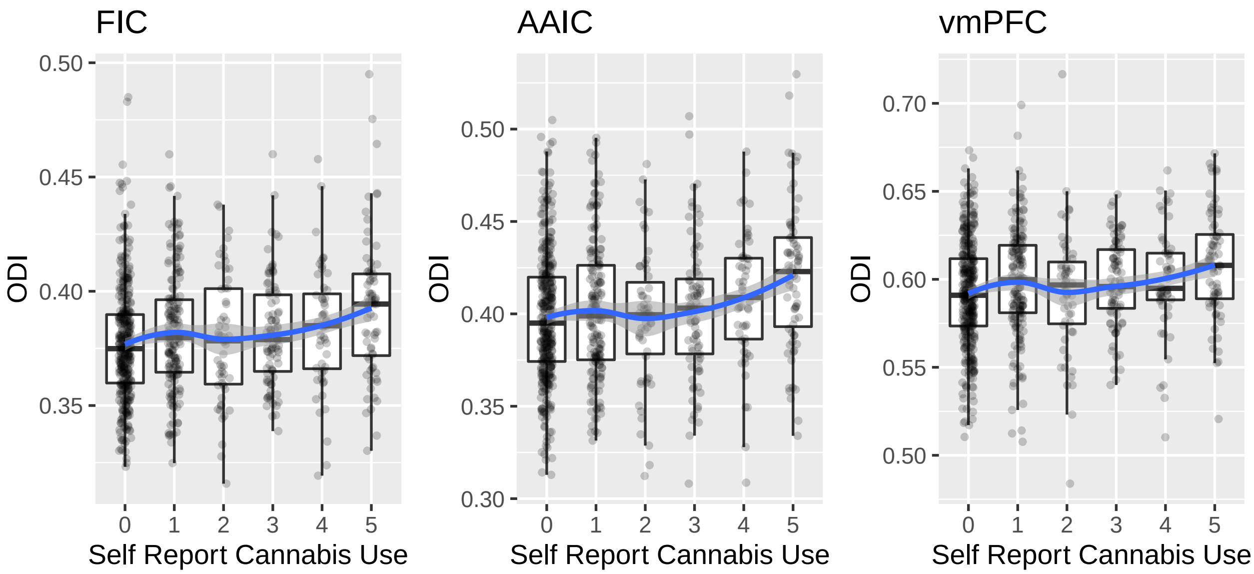

Figure 7: Plots showing associations with cortical gray matter microstructure and self reported substance abuse. Non-parametric regressions show the greatest change is at the high end.

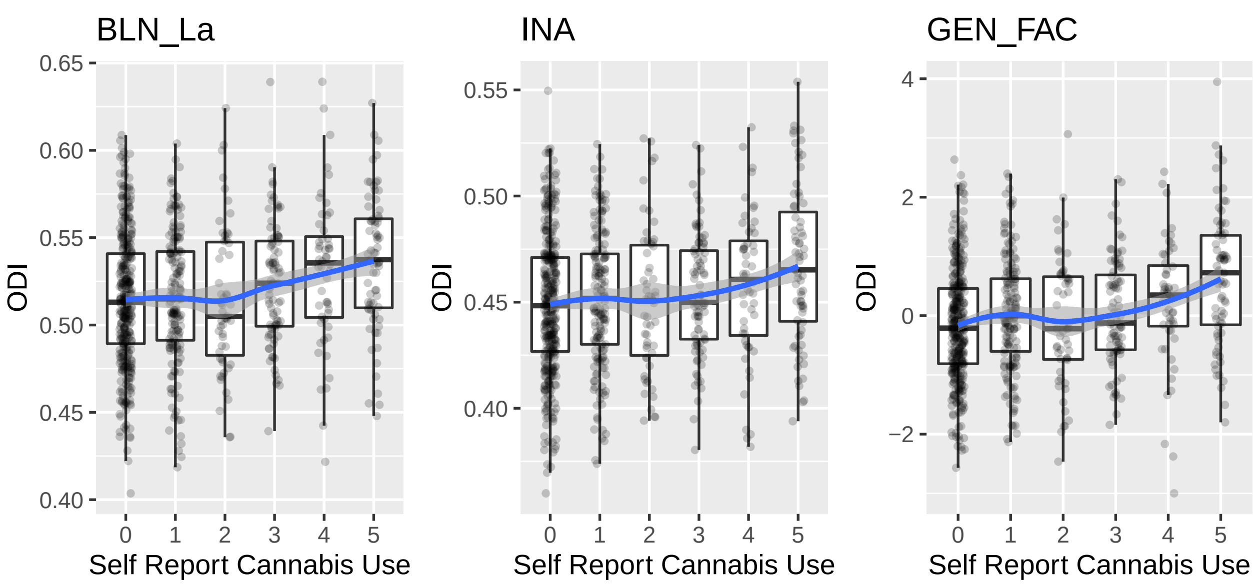

Figure 8: Plots showing associations with amygdala microstructure and self reported substance abuse. Non-parametric regressions show the greatest change is at the high end.

Plots of fractional anisotropy

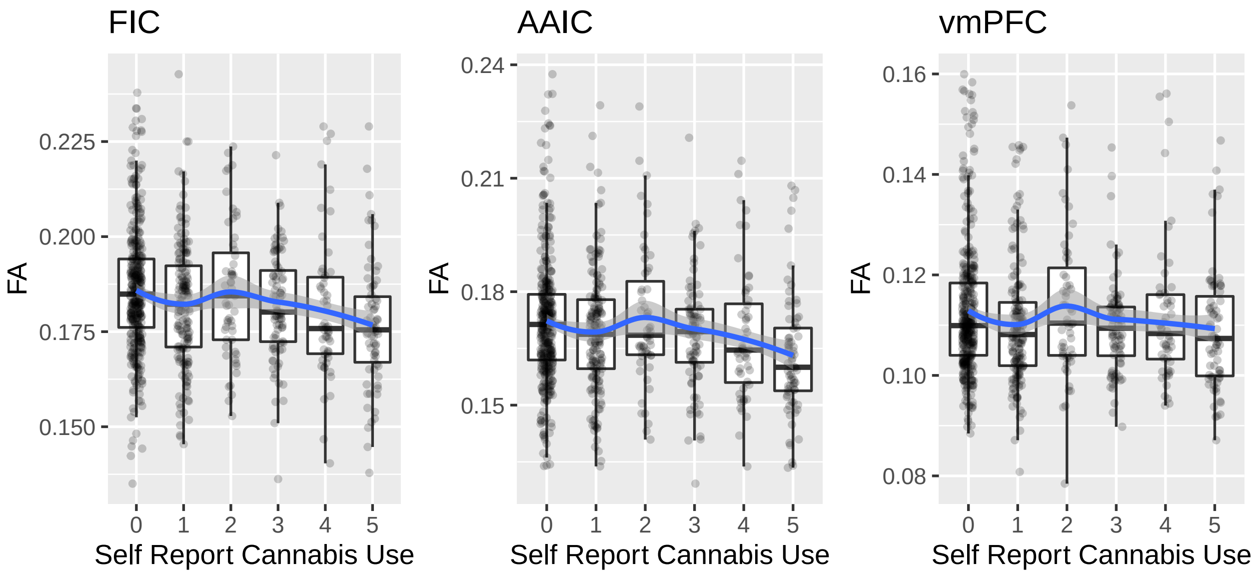

Figure 9: Plots showing associations with cortical gray matter microstructure and self reported substance abuse. Non-parametric regressions show the greatest change is at the high end.

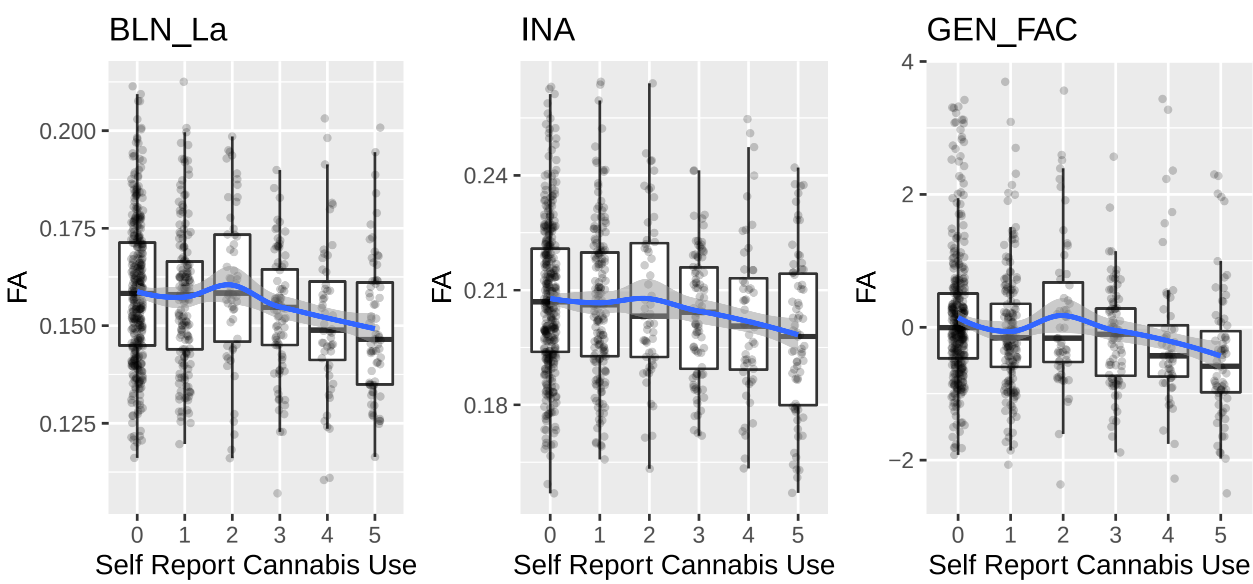

Figure 10: Plots showing associations with amygdala microstructure and self reported substance abuse. Non-parametric regressions show the greatest change is at the high end.

Behavioral characteristics in relation to THC exposure and tissue microstructure

Shown below are plots and tables comparing behavioral parameters and tissue microstructure and relating them to THC exposure. The plots show raw data comparing the general factors of ODI and FA with THC exposure, gender, body mass index (BMI), memory accuracy (MEM), negative intrusive thinking (NIT), and paternal substance abuse (PSA). The plots include jittered points for each participant and box plots to show the median and quartiles.

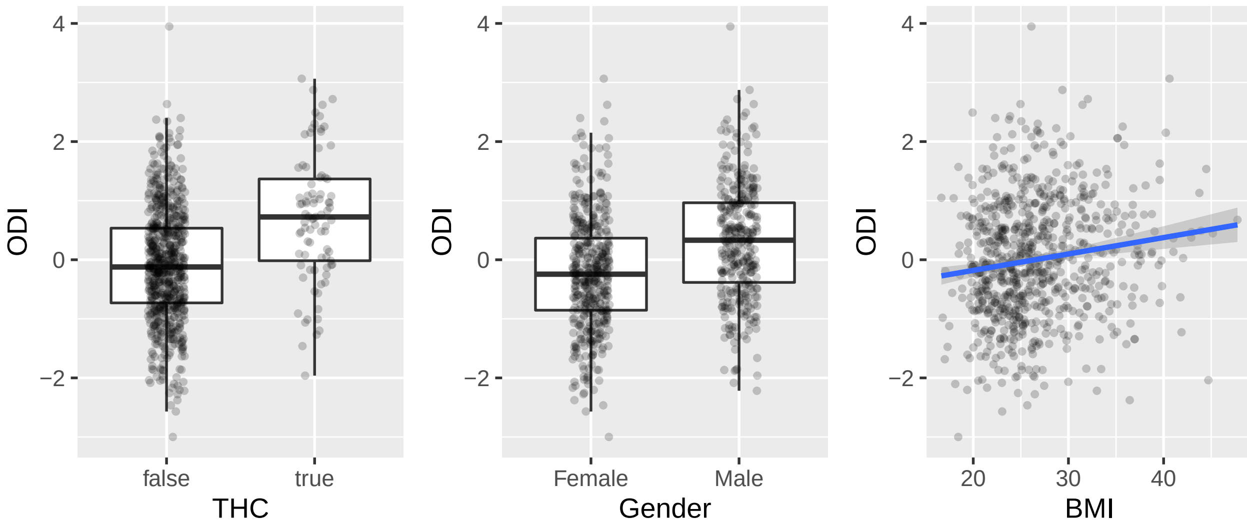

Figure 11: Plots showing the relationship between a general factor for ODI microstructure and participant demographics

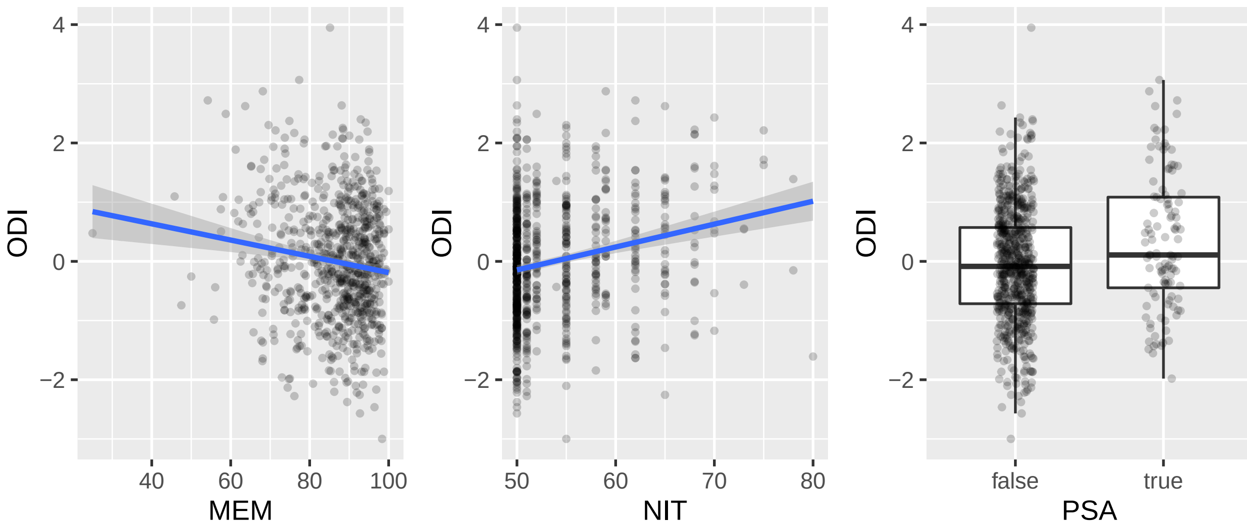

Figure 12: Plots showing the relationship between a general factor for ODI microstructure and participant demographics

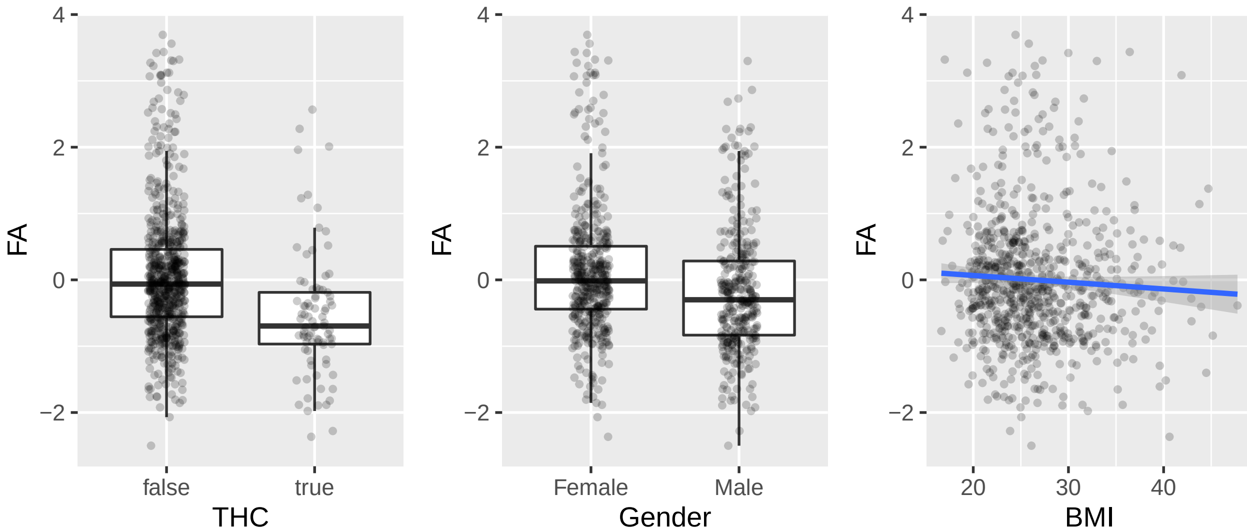

Figure 13: Plots showing the relationship between a general factor for FA microstructure and participant demographics

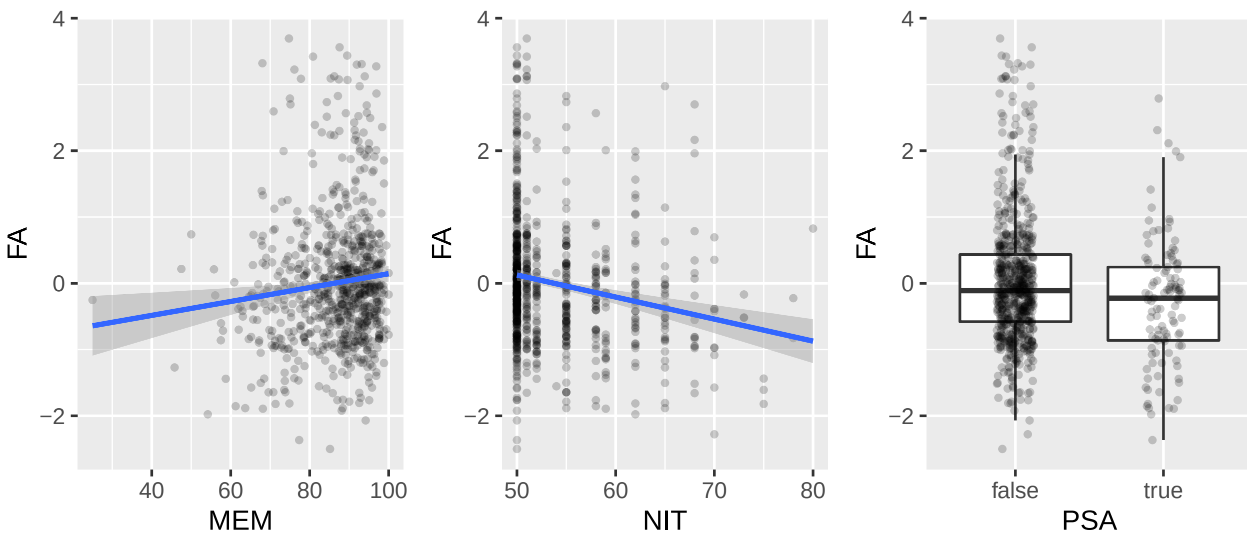

Figure 14: Plots showing the relationship between a general factor for FA microstructure and participant demographics

Relation to body mass index, smoking, and drinking

We estimated multiple linear regression models to assess the relationship between THC, microstructure and body mass index (BMI) and whether the partipant is a daily smoker (DailySmoke) or daily drinker (DailyDrink). The results show that THC has a distinct effect with these covariates, and gender had a significant effect on ODI and FA, while BMI only had a significant effect on ODI. We include separate regressions for the THC negative participants (columns two and four) for comparison.

Table 9: Multiple linear regression plots showing the relation of THC effects to BMI, smoking, and drinking. Columns two and four show results for the THC negative subset of participants.

	Dependent variable:			
	ODI_GEN_FAC		FA_GEN_FAC	
	(1)	(2)	(3)	(4)
THCtrue	0.622***		−0.471***	
	p = 0.00000		p = 0.0001	
GenderMale	0.458***	0.482***	−0.211***	−0.233***
	p = 0.000	p = 0.000	p = 0.005	p = 0.003
Age	0.061*	0.046	0.037	0.048
	p = 0.077	p = 0.198	p = 0.311	p = 0.216
BMI	0.026***	0.024***	−0.010	−0.007
	p = 0.00005	p = 0.0004	p = 0.139	p = 0.312
DailySmoke	0.023	0.011	−0.024	−0.014
	p = 0.128	p = 0.520	p = 0.138	p = 0.443
DailyDrink	0.025	0.030	−0.010	−0.011
	p = 0.193	p = 0.137	p = 0.613	p = 0.625
Constant	−1.024***	−0.981***	0.448**	0.380*
	p = 0.000	p = 0.00000	p = 0.018	p = 0.059
Observations	778	693	778	693
R^2	0.143	0.092	0.055	0.022
Adjusted R^2	0.136	0.086	0.048	0.015
Note:				*p<0.1; **p<0.05; ***p<0.01

Relation to memory, negative intrusive thinking and paternal substance abuse

We estimated a multiple linear regression model containing all relevant covariates described above, which also retained significant associations between THC and tissue microstructure. According to the R^2 coefficient, the best performing model captured approximates 18% of the variance in ODI.

Table 10: Multiple linear regression plots showing the relation of ODI THC effects to covariates. MEM performance, thought problems, and paternal substance abuse show parallel but distinct associations with gray matter microstructure

	Dependent variable:	
	ODI_GEN_FAC	FA_GEN_FAC
	(1)	(2)
THCtrue	0.426***	−0.297**
	p = 0.0003	p = 0.015
GenderMale	0.510***	−0.255***
	p = 0.000	p = 0.001
Age	0.059*	0.041
	p = 0.086	p = 0.260
BMI	0.020***	−0.005
	p = 0.002	p = 0.439
MEM	−0.107***	0.083**
	p = 0.003	p = 0.026
NIT	0.139***	−0.117***
	p = 0.0001	p = 0.002
PSAtrue	0.212**	−0.218**
	p = 0.030	p = 0.035
DailySmoke	0.011	−0.013
	p = 0.466	p = 0.423
DailyDrink	0.032*	−0.018
	p = 0.090	p = 0.375
Constant	−0.903***	0.357*
	p = 0.00000	p = 0.058
Observations	768	768
R^2	0.179	0.083
Adjusted R^2	0.169	0.072
Note:	*p<0.1; **p<0.05; ***p<0.01	

Logistic regression modeling of THC

We complemented the above models with a logistic regression model where the outcome variable was THC exposure. The results show that tissue microstructure significantly improves the predictive power of the model with a comparable effect size to previous models.

Table 11: Logistic regression models showing that a general factor of microstructure significantly improves the prediction of THC exposure

	Dependent variable:		
	THC		
	(1)	(2)	(3)
GenderMale	1.022***	0.739**	0.914***
	p = 0.0003	p = 0.012	p = 0.002
Age	−0.311**	−0.363***	−0.307**
	p = 0.020	p = 0.008	p = 0.023
BMI	−0.024	−0.033	−0.025
	p = 0.365	p = 0.226	p = 0.348
MEM	−0.379***	−0.312**	−0.333***
	p = 0.002	p = 0.013	p = 0.008
NIT	0.375***	0.304***	0.330***
	p = 0.0005	p = 0.007	p = 0.003
PSAtrue	0.533	0.378	0.452
	p = 0.106	p = 0.272	p = 0.178
DailySmoke	0.218***	0.213***	0.213***
	p = 0.00000	p = 0.00001	p = 0.00001
DailyDrink	0.101	0.096	0.097
	p = 0.146	p = 0.170	p = 0.163
ODI_GEN_FAC		0.515***	
		p = 0.0005	
FA_GEN_FAC			−0.415**
			p = 0.011
Constant	−2.820***	−2.509***	−2.779***
	p = 0.0002	p = 0.001	p = 0.0002
Observations	768	768	768
Log Likelihood	−213.318	−206.906	−209.759
Akaike Inf. Crit.	444.637	433.811	439.517
Note:			*p<0.1; **p<0.05; ***p<0.01